Inhibitions of Sugar Transport Produced by Ligands Binding at Opposite Sides of the Membrane. Evidence for Simultaneous Occupation of the Carrier by Maltose and Cytochalasin B†

Anthony Carruthers* and Amy L. Helgerson

Department of Biochemistry and Molecular Biology and Program in Molecular Medicine, University of Massachusetts Medical Center, 373 Plantation Street, Worcester, Massachusetts 01605

Received August 24, 1990; Revised Manuscript Received January 10, 1991

ABSTRACT: This study examines inhibitions of human erythrocyte D-glucose uptake at ice temperature produced by maltose and cytochalasin B. Maltose inhibits sugar uptake by binding at or close to the sugar influx site. Maltose is thus a competitive inhibitor of sugar uptake. Cytochalasin B inhibits sugar transport by binding at or close to the sugar efflux site and thus acts as a noncompetitive inhibitor of sugar uptake. When maltose is present in the uptake medium, $K_{i(app)}$ for cytochalasin B inhibition of sugar uptake increases in a hyperbolic manner with increasing maltose. When cytochalasin B is present in the uptake medium, $K_{i(app)}$ for maltose inhibition of sugar uptake increases in a hyperbolic manner with increasing cytochalasin B. High concentrations of cytochalasin B do not reverse the competitive inhibition of D-glucose uptake by maltose. These data demonstrate that maltose and cytochalasin B binding sites coexist within the glucose transporter. These results are inconsistent with the simple, alternating conformer carrier model in which maltose and cytochalasin B binding sites correspond to sugar influx and sugar efflux sites, respectively. The data are also incompatible with a modified alternating conformer carrier model in which the cytochalasin B binding site overlaps with but does not correspond to the sugar efflux site. We show that a glucose transport mechanism in which sugar influx and sugar efflux sites exist simultaneously is consistent with these observations.

The mechanism by which the family of glucopyranose transport proteins (sugar carriers or transporters) mediates the facilitated diffusion of selected sugars across cell membranes is unknown. Some studies have suggested that transport is mediated by a carrier alternating between two states in which a sugar binding site is exposed either to cytosol or to the interstitium but never to both environments simultaneously (Widdas, 1952; Krupka & Devés, 1981; Wheeler & Hinkle, 1981, 1985; Wheeler, 1986; Wheeler & Whelan, 1988; Appleman & Lienhard, 1989). We refer to this carrier as the simple or one-site carrier. Other studies have suggested that sugar transport may be mediated by a carrier that possesses multiple sugar binding sites exposed simultaneously to cytosol and interstitium (Baker & Widdas, 1973a; Naftalin & Holman, 1977; Holman, 1980; Holman et al., 1981; Naftalin et al., 1985; Carruthers, 1986a, 1989; Helgerson & Carruthers, 1987; Naftalin, 1988a,b). The simplest of these models is the two-site carrier which simultaneously presents sugar influx and efflux sites to available substrate (Baker & Widdas, 1973a; Naftalin & Holman, 1977).

Recent measurements of steady-state glucose transport in human erythrocytes suggest that the one-site carrier model may provide an adequate mathematical description of sugar transport (Wheeler, 1986; Wheeler & Whelan, 1988). However, as our previous analysis shows (Carruthers, 1991), if transport data are consistent with the one-site carrier model, they are also quantitatively consistent with the predictions of two-site carrier mechanisms.

Very few studies have attempted actively to distinguish between these models for sugar transport. Studies of ligand binding to the glucose carrier have resulted in contradictory conclusions (Jung & Rampal, 1976, 1977; Sogin & Hinkle, 1980; Gorga & Lienhard, 1981, 1982; Carruthers, 1986a,b; Helgerson & Carruthers, 1987) while pre-steady-state measurements of internal carrier relaxations have revealed an unexpected complexity in carrier function (Lowe & Walmsley, 1987; Naftalin, 1988a,b).

To date, a single study has been reported in which direct tests of the predictions of one-site and two-site carrier models have been made using steady-state sugar transport measurements (Krupka & Devés, 1981). This approach was based upon sugar efflux measurements in the simultaneous presence of two types of sugar transport inhibitors, one believed to act at or near the sugar influx site (phloretin) and the other at or near the sugar efflux site (cytochalasin B). The results of this study were consistent with the predictions of the one-site model and with those of a two-site model in which cytochalasin B and phloretin binding to the carrier display very strong negative cooperativity [$K_{d(app)}$ for cytochalasin B binding to the carrier is increased by more than 30-fold by occupation of the external site by phloretin]. Support for the latter possibility was obtained in a subsequent ligand binding study (Helgerson & Carruthers, 1987).

In this study we extend this approach to measurements of sugar uptake in the presence of cytochalasin B and maltose (an inhibitor that binds to the sugar influx site). We use maltose rather than phloretin or 4,6-*O*-ethylidene-α-D-glucopyranose. Transport inhibitions by phloretin display an unexplained complexity (K_i for phloretin inhibition of D-glucose uptake is 35-fold greater than K_i for inhibition of D-glucose efflux; Krupka, 1985), and 4,6-*O*-ethylidene-α-D-glucopyranose slowly penetrates cells to interact with the efflux site (Baker & Widdas, 1973b; Baker et al., 1978). We measure sugar transport using radiolabeled D-glucose rather than by meas-

† This work was supported by National Institutes of Health Grant DK 36081.

* Author to whom correspondence should be addressed.

0006-2960/91/0430-3907$02.50/0

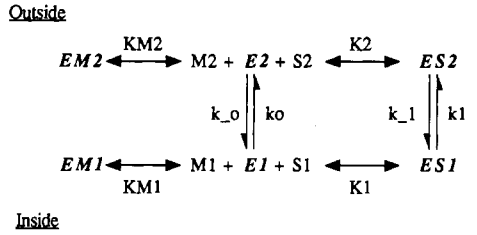

FIGURE 1: Simple one-site glucose carrier model. The carrier (E) is proposed to exist in either of two possible states in the absence of transportable sugar (S) or transport inhibitors (M). The E_1 state presents a sugar binding site to the cell's interior while the E_2 state presents a sugar site to the cell's exterior. These two states are mutually exclusive and isomerize at rates described by the first-order rate constants k_0 and k_{-0}. The carrier binds intra- or extracellular sugars (S_1 or S_2, respectively) but not both simultaneously. The E_1 isomer reacts with either S_1 or transport inhibitors that bind exclusively to E_1 (M_1). The EM_1 complex is a dead-end complex while the ES_1 complex isomerizes to ES_2 (described by the first-order rate constant k_1). The E_2 isomer reacts with either S_2 or with transport inhibitors (M_2) that bind exclusively to E_2. The EM_2 complex is a dead-end complex while the ES_2 complex isomerizes to ES_1 (described by the first order rate constant k_{-1}).

uring transport-induced changes in cell volume (Krupka & Devês, 1981). We develop an analysis of theoretical one- and two-site carrier-mediated sugar transport inhibitions by maltose and cytochalasin B and show that these models may be distinguished using steady-state transport measurements.

We conclude that the glucose carrier maltose and cytochalasin B binding sites exist simultaneously. These findings demonstrate that transport inhibitions produced by maltose and cytochalasin B together are irreconcilable with the predictions of the classical one-site carrier model for transport.

THEORY

We consider three theoretical models for the facilitated diffusion of sugars across the cell membrane. The one-site carrier model is the classical "mobile carrier" model first proposed by Widdas (1952) and is shown in King–Altman form in Figure 1 (see legend for details).

Assuming that binding of S and M occurs more rapidly than carrier isomerizations (Lowe & Walmsley, 1986), this scheme can be solved for sugar uptake in the presence of inhibitors M_1 and M_2. Uptake, v_{21}, is given by

$$v_{21} = \frac{S_2(K + S_1)}{K^2R_{oo} + KR_{21}S_2 + KR_{12}S_1 + R_{ee}S_1S_2} \quad (1)$$

where

$$K = \frac{K_1k_0}{k_1} = \frac{K_2k_{-0}}{k_{-1}}$$

$$R_{oo} = \frac{k_{-0}\left(1 + \frac{M_1}{K_{M_1}}\right) + k_0\left(1 + \frac{M_2}{K_{M_2}}\right)}{k_0k_{-0}}$$

$$R_{21} = \frac{k_0 + k_{-1}\left(1 + \frac{M_1}{K_{M_1}}\right)}{k_{-1}k_0}$$

$$R_{12} = \frac{k_{-0} + k_1\left(1 + \frac{M_2}{K_{M_2}}\right)}{k_1k_{-0}}$$

$$R_{ee} = \frac{k_{-1} + k_1}{k_{-1}k_1}$$

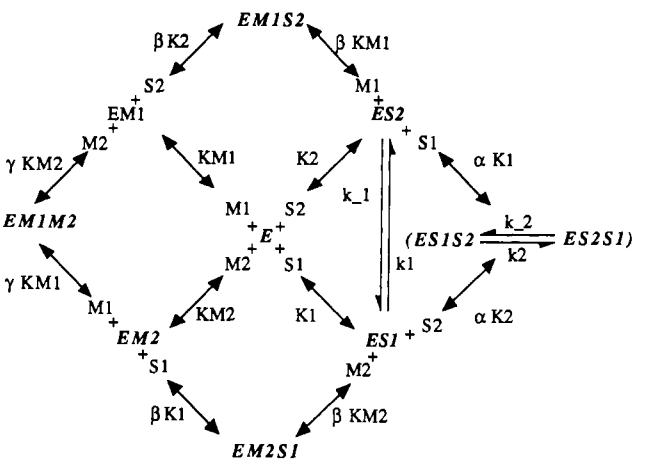

FIGURE 2: Two-site glucose carrier model. The carrier, E, can bind sugar molecules simultaneously at sugar influx and efflux sites to form a ternary complex ES_1S_2. Exchange transport (described by the first-order rate constants k_2 and k_{-2}) is presumed to involve internal subunit exchange of sugars while net transport (described by rate constants k_1 and k_{-1}) can occur in the absence of trans sugar. The inhibitors M_1 and M_2 interact with this transport system in the absence of transported sugar S to form EM_1, EM_2, and EM_1M_2 complexes. The cooperativity factor γ is included in dissociation constants describing binding of a trans inhibitor to an EM complex to allow for the possibility of cooperativity between binding sites. Similarly, binding of transportable sugars may display cooperativity; thus the cooperativity factor α is included in dissociation constants describing the binding of a trans sugar to an ES complex. When both S and M are present, heterocomplexes may be formed. It is assumed that all complexes containing both S and M are catalytically inactive, and the cooperativity factor β is included for binding of trans S or trans M to the complexes EM and ES, respectively. There is no a priori reason to assume that $\alpha = \beta = \gamma$.

S_1 and S_2 refer to the concentrations of S at sides 1 and 2 of the membrane, and M_2 and M_1 refer to concentrations of M_2 and M_1, respectively, at sides 2 and 1 of the membrane, respectively. K_2, K_{M_2}, and K_{M_1} refer to dissociation constants for binding of S_2, M_2, and M_1 to E_2, E_2, and E_1, respectively.

In the absence of S_1, zero-trans uptake of S_2 is given by

$$v_{21} = \frac{V_{21}^{zt}S_2}{K_{21}^{zt} + S_2} \quad (2)$$

where

$$V_{21}^{zt} = \frac{1}{R_{21}} = \frac{k_0k_{-1}}{k_0 + k_{-1}\left(1 + \frac{M_1}{K_{M_1}}\right)} \quad (3)$$

and

$$K_{21}^{zt} = \frac{KR_{oo}}{R_{21}} = \frac{K_2\left[k_0\left(1 + \frac{M_2}{K_{M_2}}\right) + k_{-0}\left(1 + \frac{M_1}{K_{M_1}}\right)\right]}{k_0 + k_{-1}\left(1 + \frac{M_1}{K_{M_1}}\right)} \quad (4)$$

The apparent dissociation constant for M_2 binding to the carrier [$K_{M_2(app)}$ and, because the analysis assumes rapid equilibrium kinetics, the inhibitory constant $K_{i(app)M_2}$ for transport inhibition] is given by

$$K_{M_2(app)} = \frac{K_{M_2}}{k_0}\left[k_0 + k_{-0} + \frac{S_2}{K_2}(k_0 + k_{-1}) + \frac{M_1}{K_{M_1}}\left(k_{-0} + k_{-1}\frac{S_2}{K_2}\right)\right] \quad (5)$$

and the apparent dissociation constant for M_1 binding to the carrier [$K_{M_1(app)}$ and $K_{i(app)M_1}$] is given by

$$K_{M_1(app)} = \frac{K_{M_1}\left[k_{-0} + k_0 + \frac{S_2}{K_2}(k_0 + k_{-1}) + k_0\frac{M_2}{K_{M_2}}\right]}{k_{-0} + k_{-1}\frac{S_2}{K_2}} \quad (6)$$

Thus M_2 is expected to behave as a competitive inhibitor of uptake of S_2 (increases K_{21}^{zt}) while M_1 behaves as a noncompetitive inhibitor of S_2 uptake (reduces V_{21}^{zt}).

The two-site carrier model for sugar transport proposed by Baker and Widdas (1973a) is shown in King–Altman form in Figure 2 (see legend for details). Whereas the one-site carrier model allows for the possibility of 6 carrier species in the presence of S and M, the two-site model allows for the possibility of 9 carrier species. In order to simplify the analysis, we assume that all translocation steps are slow relative to substrate binding steps and that the various carrier/sugar/inhibitor complexes are in true equilibrium with free S and M in the microenvironment surrounding binding sites.

Two-site carrier-mediated sugar uptake (v_{21}) in the presence of transport inhibitors M_1 and M_2 is given by eq 1, where

$$K = \frac{k_{-1}\alpha K_1}{k_{-2} + k_2}$$

$$R_{oo} = \frac{K_2\left(1 + \frac{M_1}{K_{M_1}} + \frac{M_1}{K_{M_2}} + \frac{M_1M_2}{\gamma K_{M_1}K_{M_2}}\right)(k_{-2} + k_2)}{\alpha K_1 k_{-1} k_{-1}}$$

$$R_{21} = \frac{1 + \frac{M_1}{\beta K_{M_1}}}{k_{-1}} \qquad R_{12} = \frac{K_2\left(1 + \frac{M_2}{\beta K_{M_2}}\right)}{K_1 k_{-1}}$$

$$R_{ee} = \frac{2}{k_{-2} + k_2}$$

In the absence of S_1, zero-trans uptake of S_2 is given by eq 2, where

$$V_{21}^{zt} = \frac{1}{R_{21}} = \frac{k_{-1}}{1 + \frac{M_1}{\beta K_{M_1}}} \quad (7)$$

and

$$K_{21}^{zt} = \frac{KR_{oo}}{R_{21}} = \frac{K_2\left(1 + \frac{M_1}{K_{M_1}} + \frac{M_2}{K_{M_2}} + \frac{M_1M_2}{\gamma K_{M_1}K_{M_2}}\right)}{1 + \frac{M_1}{\beta K_{M_1}}} \quad (8)$$

The apparent dissociation constant for M_2 binding to the two-site carrier [$K_{M_2(app)}$ and, because the analysis assumes rapid equilibrium kinetics, the inhibitory constant $K_{i(app)M_2}$ for transport inhibition] is given by

$$K_{M_2(app)} = \frac{K_{M_2}\left(1 + \frac{M_1}{K_{M_1}} + \frac{S_2}{K_2} + \frac{S_2M_1}{\beta K_2 K_{M_1}}\right)}{1 + \frac{M_1}{\gamma K_{M_1}}} \quad (9)$$

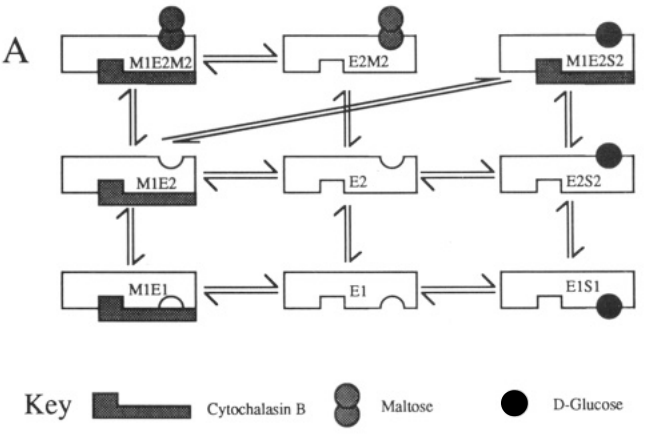

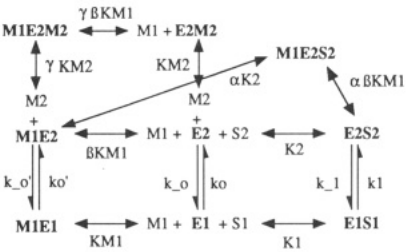

FIGURE 3: Modified one-site glucose carrier model. This model differs from the simple one-site mechanism in one aspect alone. Here it is assumed that while the maltose (M_2) binding site corresponds to the sugar influx site, the cytochalasin B (M_1) binding site overlaps with but does not correspond stereochemically to the sugar efflux site. Thus M_1 and S_1 compete for binding to E_1 but not necessarily at the same site. One method of visualizing this is shown in schematic form in panel A. The active center of the carrier is shown to contain mutually exclusive sugar influx and efflux sites but also to contain an omnipresent cytochalasin B binding site which overlaps with the intracellular sugar (S_1) binding site. The model allows for isomerization of influx and efflux sites even when the carrier is occupied by cytochalasin B. In all other regards, this model is identical with the simple one-site carrier mechanism. (B) King–Altman representation of the modified one-site carrier model. α, γ, and β cooperativity constants are included to allow for the possibility that M_1 binding to the binary complexes $E_2{\cdot}S_2$ and $E_2{\cdot}M_2$, respectively, and to E_2 may occur with higher or lower affinity than to the E_1 conformation of the carrier.

and the apparent dissociation constant for M_1 binding to the carrier [$K_{M_1(app)}$ and $K_{i(app)M_1}$] is given by

$$K_{M_1(app)} = \frac{K_{M_1}\left(1 + \frac{M_2}{K_{M_2}} + \frac{S_2}{K_2}\right)}{1 + \frac{M_2}{\gamma K_{M_2}} + \frac{S_2}{\beta K_2}} \quad (10)$$

The fundamental difference between equations describing $K_{(app)}$ for M_1 and M_2 binding to one- and two-site carrier models is the inclusion of a trans inhibitor term in the denominators of the two-site equations.

A critical factor in determining the effects of inhibitors on two-site carrier-mediated transport is the value of the cooperativity factors β and γ. γ describes interactions between the internal and external binding sites when they are occupied by nontransported inhibitors. When $\gamma < 1$, these sites display positive cooperativity, and when $\gamma > 1$, these sites display negative cooperativity. β describes interactions between the internal and external binding sites when one site is occupied by a transported sugar and the second by a nontransported inhibitor. When $\beta < 1$, these sites display positive cooperativity, and when $\beta > 1$, these sites display negative coopera-

tivity. Table I summarizes computations of M_1 and M_2 effects on $K_{m(app)}$ and V_{max} for D-glucose uptake by a two-site carrier under conditions where β and γ range from 0.01 to 100. These results are contrasted with the predicted results for one-site carrier-mediated D-glucose transport by human red cells at 0 °C.

A modified one-site carrier mechanism is shown in Figure 3. This model differs fundamentally from the simple one-site carrier in one aspect alone. Here it is assumed that the cytochalasin B binding site overlaps with but does not correspond to the sugar efflux site. However, the extracellular maltose binding site is assumed to correspond stereochemically to the extracellular sugar binding site. Since occupation of E_1 by M_1 (cytochalasin B) precludes binding of S_1 and occupation of E_1 by S_1 prevents binding of M_1, M_1 and S_1 serve as simple competitive inhibitors of S_1 and M_1 binding, respectively. M_1 and S_1 binding are mutually exclusive and thus satisfy the requirements of competitive interaction. The model as outlined thus permits simultaneous occupation of the carrier by M_1 and S_2 and by M_1 and M_2 and allows for cooperativity in binding as shown by the cooperativity factors α, β, and γ. In addition, the isomerization of E_1 to E_2 is shown to occur even when the carrier is occupied by M_1 although the rates of these isomerizations are determined by the values assigned to the rate constants k_0' and k_{-0}'.

Modified one-site carrier-mediated sugar uptake in the presence of transport inhibitors M_1 and M_2 is given by eq 1, where

$$K = \frac{\left(k_0'\frac{M_1}{\beta K_{M_1}} + k_0\right)K_1}{k_1}$$

$$R_{\infty} = K_2k_1\left\{k_{-0}\left[1 + \frac{M_1}{K_{M_1}}\left(1 + \frac{M_1}{\beta K_{M_1}}\right)\right] + k_{-0}'\frac{M_1}{\beta K_{M_1}} + \left(k_0'\frac{M_1}{\beta K_{M_1}} + k_0\right)\left(1 + \frac{M_1}{\beta K_{M_1}} + \frac{M_2}{K_{M_2}} + \frac{M_1M_2}{\beta\gamma K_{M_1}K_{M_2}}\right)\right\} \Big/ K_1k_{-1}\left(k_0'\frac{M_1}{\beta K_{M_1}} + k_0\right)^2$$

$$R_{21} = \frac{1}{V_{21}^{zt}} = \left[k_0\left(1 + \frac{M_1}{\alpha\beta K_{M_1}}\right) + k_0'\frac{M_1}{K_{M_1}}\left(1 + \frac{M_1}{\alpha\beta K_{M_1}}\right) + k_{-1}\left(1 + \frac{M_1}{K_{M_1}}\right)\right] \Big/ \left[k_{-1}\left(k_0'\frac{M_1}{\beta K_{M_1}} + k_0\right)\right] \quad (11)$$

$$R_{12} = K_2\left\{k_{-0}\left(1 + \frac{M_1}{\beta K_{M_1}}\right) + k_1\left[1 + \frac{M_2}{K_{M_2}} + \frac{M_1}{\beta K_{M_1}}\left(1 + \frac{M_2}{\gamma K_{M_2}}\right)\right]\right\} \Big/ \left[K_1k_{-1}\left(k_0'\frac{M_1}{\beta K_{M_1}} + k_0\right)\right]$$

$$R_{ee} = \frac{1}{V^{ee}} = \frac{k_{-1} + k_1\left(1 + \frac{M_1}{\alpha\beta K_{M_1}}\right)}{k_1k_{-1}} \quad (12)$$

where V^{ee} is the maximum velocity of equilibrium exchange ($S_1 = S_2$ = saturating) sugar transport. When $M_1 = M_2 = 0$, the various transport constants reduce to the forms expected of the simple one-site carrier (see above).

The apparent dissociation constant for M_2 binding to the carrier [$K_{M_2(app)}$ and, because the analysis assumes rapid equilibrium kinetics, the inhibitory constant $K_{i(app)M_2}$ for transport inhibition] is given by

$$K_{M_2(app)} = \frac{K_{M_2}\left(\frac{M_1}{K_{M_1}}N_1 + k_0 + k_{-0} + \frac{S_2}{K_2}N_2\right)}{k_0'\frac{M_1}{K_{M_1}}\left(1 + \frac{M_1}{\beta\gamma K_{M_1}}\right) + k_0\left(1 + \frac{M_1}{\beta\gamma K_{M_1}}\right)} \quad (13)$$

where

$$N_1 = k_0'\left(1 + \frac{M_1}{\beta K_{M_1}}\right) + \frac{1}{\beta}(k_0 + k_{-0}') + k_{-0}\left(1 + \frac{M_1}{\beta K_{M_1}}\right)$$

and

$$N_2 = k_0'\frac{M_1}{K_{M_1}}\left(1 + \frac{M_1}{K_{M_1}}\right) + k_0\left(1 + \frac{M_1}{\alpha\beta K_{M_1}}\right) + k_{-1}\left(1 + \frac{M_1}{K_{M_1}}\right)$$

Equations 5 and 13 reduce to the same form when $M_1 = 0$, namely

$$K_{M_2(app)} = \frac{K_{M_2}\left[k_0 + k_{-0} + \frac{S_2}{K_2}(k_0 + k_{-1})\right]}{k_0}$$

Using eq 13, it is possible to model the data of Figure 6B according to a modified one-site carrier only with the following conditions: $k_0' = k_0$, $k_{-0}' = k_{-0}$, $\alpha \to \infty$, $\beta < 1$, and $\gamma \approx 10$. Interpretation of these constants within this context indicates that isomerization of the unoccupied sugar binding sites is unaffected by occupation of the carrier by M_1; the ternary complex $M_1{\cdot}E_2{\cdot}S_2$ cannot exist; M_1 binding to E_2 occurs with greater affinity than does M_1 binding to E_1; binding of M_1 and M_2 to E_2 to form the ternary complex $M_1{\cdot}E_2{\cdot}M_2$ displays negative cooperativity.

As cytochalasin B is a competitive inhibitor of equilibrium exchange transport [V^{ee} is unaffected by M_1 (Basketter & Widdas, 1978)], it seems justifiable to assign a value of infinity to α (see eq 12). However, examination of eq 11 shows that the only means of forcing linear, noncompetitive inhibition of S_2 uptake by M_1 (see Figure 4B) to assign a value of infinity to the parameter β. Under these conditions, M_1 is without effect on $K_{M_2(app)}$. When $\beta \leq 1$, R_{21} falls with increasing M_1; thus V_{21}^{zt} for S_2 uptake is increased by M_1. As cytochalasin B (M_1) is a noncompetitive inhibitor of D-glucose uptake and a competitive inhibitor of equilibrium exchange transport, we are forced to reject the modified one-site carrier as an appropriate model for erythrocyte sugar transport inhibitions by maltose and cytochalasin B.

Materials and Methods

Reagents. [U-^{14}C]-D-Glucose and [^{3}H]cytochalasin B were purchased from New England Nuclear. Cytochalasin B, phloretin, D-glucose, and maltose were purchased from Sigma Chemicals. All other reagents were purchased from either Sigma Chemicals or Fisher.

Table I: Predicted Effects of Inhibitors Acting at Opposite Sides of the Membrane on Michaelis and Velocity Parameters for Human Red Cell D-Glucose Uptake

	one-site carrier[a]		two-site carrier[b]		
inhibitors[c]	K_{21}^{zt} [d]	V_{21}^{zt} [e]	K_{21}^{zt} [d]	V_{21}^{zt} [e]	comments[f]
M_1	no change	decrease	no change	decrease	$\beta = \gamma = 1$
M_2	increase	no change	increase	no change	$\beta = \gamma = 1$
$M_1 + M_2$	no change	decrease	increase	decrease	$\beta = \gamma = 1$
$M_1 + M_2$			decrease	decrease	$\beta \ll 1; \gamma = 1$
$M_1 + M_2$			increase	decrease	$\beta \gg 1; \gamma = 1$
$M_1 + M_2$			increase	decrease	$\beta = 1; \gamma \ll 1$
$M_1 + M_2$			increase	decrease	$\beta = 1; \gamma \gg 1$
$M_1 + M_2$			increase	decrease	$\beta \ll 1; \gamma \ll 1$
$M_1 + M_2$			decrease	decrease	$\beta \ll 1; \gamma \gg 1$
$M_1 + M_2$			increase	decrease	$\beta \gg 1; \gamma \ll 1$
$M_1 + M_2$			increase	decrease	$\beta \gg 1; \gamma \gg 1$

[a] The results for the one-site carrier are predicted from eqs 2 and 3 by using values for k_0, k_{-0}, k_{-1}, and K_2 of 0.0048 s^{-1}, 0.089 s^{-1}, 8.2 s^{-1}, and 10 mM, respectively (Lowe & Walmsley, 1986). $E_t \approx 4.2$ μM. [b] The results for the two-site carrier are predicted from eqs 7 and 8 by using values of k_{-1} and K_2 of 0.0048 s^{-1} and 0.115 mM, respectively. $E_t \approx 4.2$ μM. [c] Inhibitors refer to concentrations of inhibitor (M) present at side 1 (cytosolic) or side 2 (extracellular) of the red cell membrane where $[M]/K_M = 10$. [d] K_{21}^{zt} refers to $K_{m(app)}$ for D-glucose uptake. [e] V_{21}^{zt} refers to V_{max} for D-glucose uptake. [f] Assignments to the cooperativity factors β and γ where $\ll 1 = 1/100$ and $\gg 1 = 100$.

Solutions. Saline contained NaCl (150 mM), EDTA[1] (0.5 mM), and HEPES (5 mM) adjusted to pH 7.4 (24 °C) with NaOH. Stopper contained NaCl (150 mM), HEPES (5 mM), KI (1.5 mM), $HgCl_2$ (10 μM), phloretin (100 μM), and cytochalasin B (50 μM) adjusted to pH 7.4 (24 °C) with NaOH. Cytochalasin B and phloretin were added to stopper immediately prior to use, and then the solution was cooled to ice–water temperature (0–2 °C). All solutions were adjusted to 0.1% (v/v) dimethyl sulfoxide (the carrier for cytochalasin B).

Most of the experiments reported in this study were carried out in the presence of 0–190 mM maltose. To avoid cell volume induced artifacts, maltose-free saline contained 190 mM sucrose. As the maltose concentration was increased, a corresponding decrease in sucrose concentration was made. Thus, assuming the activity coefficients of maltose and sucrose are identical, all cells were exposed to media of identical osmolality. In these experiments sucrose (190 mM) was added to stopper solutions.

Preparation of Red Cells. Human red cells were collected from recently expired, whole human blood (University of Massachusetts Medical Center Blood Bank) by suspension in ice-cold saline (10 volumes of saline:1 volume of whole blood) followed by centrifugation at 25000*g* for 10 min. The supernatant and buffy coat were aspirated, and the red cell pellet was resuspended in saline. This wash/centrifugation procedure was repeated until the supernatant was clear and the red cell pellet lacked any discernible buffy coat (normally three to four cycles). The washed red cells were then resuspended in 100 volumes of saline and allowed to rest at room temperature for 1 h to deplete cells of intracellular D-glucose. The D-glucose-depleted cells were then harvested by centrifugation to a final hematocrit of 80–90%.

Measurement of Zero-Trans D-*Glucose Uptake.* All uptake measurements were made at ice–water temperature (0–2 °C). All solutions, glassware, plasticware, and cell preparations were equilibrated to this temperature for at least 30 min prior to the initiation of uptake measurements. Cells were preequilibrated ± inhibitors (cytochalasin B and maltose as appropriate) for 20 min prior to the addition of uptake medium (unlabeled and labeled D-glucose ± appropriate inhibitors). Additions of D-glucose did not alter total concentrations of inhibitors.

Transport measurements were carried out as follows. At zero time 150 μL of uptake medium was added to 10 μL of a 50% suspension of red cells in appropriate preequilibration medium (e.g., containing or lacking sucrose/maltose and/or cytochalasin B). Following the desired time interval, 1.25 mL of stopper was added. The cells were immediately collected by centrifugation at 14000*g* for 20 s, resuspended in 1.25 mL of stopper, centrifuged for a second time, and then extracted in 250 μL of 3% trichloroacetic acid. The extracted suspension was centrifuged (20 s at 14000*g*), and 2 × 100 μL aliquots of the clear supernatant were counted by liquid scintillation spectrometry.

Zero-time uptake measurements were made by first adding stopper to the cells (10 μL of 50% suspension) followed by addition of 150 μL of uptake medium. The cells were then processed as described above. Equilibrium uptake measurements are not feasible using D-glucose owing to appreciable (33%) metabolism of labeled D-glucose at low (<1 mM) total D-glucose levels following incubation for 1 h at 37 °C (not shown). Uptake was normalized to uptake per 1.7×10^{13} cells (that number of cells containing 1 L of water under normosmotic conditions) or to uptake per 2.8×10^{13} cells (that number of cells in saline plus 200 mM sucrose or maltose containing 1 L of water) by counting the number of cells per uptake reaction with a hemacytometer.

The rate of D-glucose uptake (v_{21}) was calculated as

$$v_{21} = \frac{2.5(\text{cpm}_t - \text{cpm}_0)QC}{C_n t}$$

where cpm_t and cpm_0 refer to radioactivity associated with the cells at time t and zero time, respectively, Q is the number of moles of D-glucose per cpm present in uptake medium, C refers to 1.7×10^{13} or to 2.8×10^{13} cells as appropriate, and C_n is the number of cells present in each uptake reaction mixture.

Uptake of D-glucose was measured over intervals as short as 5 s to intervals as long as 20 min. In all cases, "initial rates" of uptake were calculated from measurements in which the D-glucose space of the cells was never greater than 15% of the water space (assuming that 1.7×10^{13} cells suspended in saline contain 1 L of water and that 2.8×10^{13} cells suspended in saline containing 200 mM maltose or sucrose contain 1 L of water). Our experiments indicate that, in the absence of maltose and cytochalasin B, $K_{m(app)}$ and V_{max} for D-glucose uptake are 0.069 mM and 89 μM/min, respectively. Thus at limitingly low D-glucose, the rate constant for D-glucose uptake is ≈ 1.3 min^{-1} $[V_{max}/K_{m(app)}]$, which corresponds to a half-time

[1] Abbreviations: EDTA, ethylenediaminetetraacetic acid; HEPES, *N*-(2-hydroxyethyl)piperazine-*N*′-2-ethanesulfonic acid; $K_{i(app)}$, apparent inhibitory constant; $K_{m(app)}$, apparent Michaelis constant for sugar uptake.

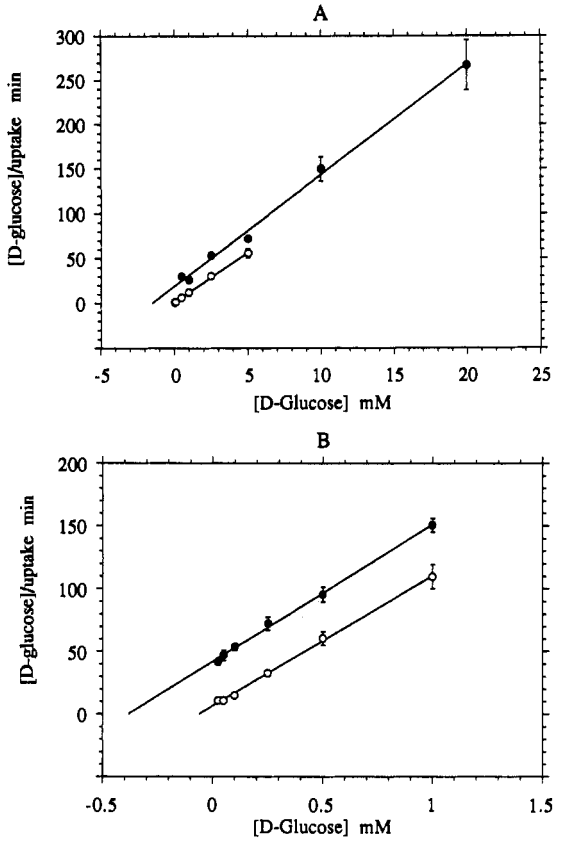

FIGURE 4: D-Glucose dependence of zero-trans D-glucose uptake by human erythrocytes. (A) Effects of maltose on D-glucose uptake in the absence of cytochalasin B. The data are presented as a Hanes–Woolf plot. Ordinate: [D-glucose]/rate of D-glucose uptake in min (assuming 2.8×10^{13} cells suspended in saline + 200 mM maltose or sucrose contain 1 L of water). Abscissa: D-glucose concentration in mmol·L^{-1}. Uptake in the absence of maltose is shown by the open circles (○) and in the presence of 200 mM maltose by the filled circles (●). The number of duplicate measurements per data point is 3 or more. Each point represents the calculated mean ± 1 standard error. The straight lines drawn through the points were calculated by the method of least squares. The following constants characterize D-glucose uptake. Control: $K_{m(app)}$ = 0.069 mM, V_{max} = 89.3 μmol·(2.8 × 10^{13} cells)$^{-1}$·min^{-1}. Maltose: $K_{m(app)}$ = 1.496 mM, V_{max} = 80.1 μmol·(2.8 × 10^{13} cells)$^{-1}$·min^{-1}. (B) Effects of maltose on D-glucose uptake in the presence of cytochalasin B (998 ± 24 nM). Ordinate and abscissa as in (A). Uptake in the absence of maltose is shown by the open circles (○) and in the presence of 200 mM maltose by the filled circiles (●). The number of duplicate measurements per data point is 3 or more. Each point represents the calculated mean ± 1 standard error. The straight lines drawn through the points were calculated by the method of least squares. The following constants characterize D-glucose uptake. Control: $K_{m(app)}$ = 0.060 mM, V_{max} = 9.6 μmol·(2.8 × 10^{13} cells)$^{-1}$·min^{-1}. Maltose: $K_{m(app)}$ = 0.38 mM, V_{max} = 9.1 μmol·(2.8 × 10^{13} cells)$^{-1}$·min^{-1}.

for equilibration of 0.54 min assuming monoexponential uptake of sugar. This means that at 5 s, the cells are no more than 10% equilibrated with subsaturating extracellular sugar.

Cytochalasin B Concentrations. Owing to the large cytochalasin B binding capacity of human red cells and the speed of cytochalasin B binding to these cells (Helgerson & Carruthers, 1987), the total cytochalasin B concentrations present in the uptake media do not accurately reflect the free cytochalasin B concentrations present in the medium. In experiments where transport inhibitions were measured in the presence of cytochalasin B, free cytochalasin B was measured in parallel by using [^{3}H]cytochalasin B. Tracer [^{3}H]cytochalasin B was added to each uptake tube (in the absence of labeled D-glucose, but in the presence of appropriate cytochalasin B, D-glucose, and maltose levels), and aliquots (2 × 10 μL) of the suspension were sampled. The cells were then sedimented by centrifugation, and aliquots (2 × 10 μL) of the supernatant were sampled. Following trichloroacetic acid extraction (see above), the samples were counted. Free [cytochalasin B] was calculated as

$$[\text{cytochalasin B}]_{free} = \frac{[\text{cytochalasin B}]_{total}\text{cpm}_{sn}}{\text{cpm}_{total}}$$

where cpm_{sn} and cpm_{total} refer to cpm present in supernatant and suspension samples, respectively. A detailed description of this methodology is provided in Helgerson and Carruthers (1987).

Calculation of Michaelis and Velocity Parameters for Sugar Uptake. "Initial rates" of transport were calculated from at least two incubation intervals (where v_{21} was independent of time) at each [D-glucose] employed; at least six concentrations of [D-glucose] which, based upon preliminary experiments, span the range [D-glucose] ≥ $K_{m(app)}/5$ to [D-glucose] ≤ $10K_{m(app)}$ were used. The [D-glucose]/velocity data were analyzed by linearization (Hanes–Woolf plot of [D-glucose]/uptake versus [D-glucose]) to obtain estimates of K_{21}^{zt} and V_{21}^{zt}. Linear regression and nonlinear regression analyses (weighted and unweighted) were performed by using the software package KaleidaGraph 2.1 (Synergy Software, Reading, PA).

RESULTS

Dependence of D-Glucose Uptake on D-Glucose Concentration. Figure 4 shows that D-glucose uptake by erythrocytes at ice–water temperature is well approximated by simple saturation kinetics. $K_{m(app)}$ and V_{max} for D-glucose uptake are 69 μM and 89.3 μmol·(L of cell water)$^{-1}$·min^{-1}, respectively.

Nature of Transport Inhibitions Produced by Maltose and Cytochalasin B. Maltose increases $K_{m(app)}$ for D-glucose uptake (V_{max} is unchanged) while cytochalasin B acts to reduce V_{max} for sugar uptake [$K_{m(app)}$ is unchanged; Figure 4]. These inhibitions suggests that maltose acts as a competitive inhibitor of D-glucose uptake while cytochalasin B acts as a noncompetitive inhibitor of transport. $K_{i(app)}$ values for maltose and cytochalasin B inhibitions of D-glucose uptake in these experiments are 9.7 mM and 126 nM, respectively.

Inhibitions of Transport Produced by Simultaneous Presence of Maltose and Cytochalasin B. Figure 5 summarizes an experiment in which 0.1 mM D-glucose uptake was measured in the presence of both maltose (0–150 mM) and cytochalasin B (0–1980 nM). The results of this single experiment demonstrate that $K_{i(app)}$ for cytochalasin B inhibition of transport increases nonlinearly with [maltose] and that $K_{i(app)}$ for maltose inhibition of transport increases nonlinearly with [cytochalasin B]. Figure 6 summarizes the results of five similar experiments.

Effects of Simultaneous Presence of Maltose and Cytochalasin B on the Dependence of D-Glucose Uptake on D-Glucose Concentration. Figure 4 shows the concentration dependence of D-glucose uptake in the presence of both maltose (0 and 200 mM) and cytochalasin B (998 nM). $K_{m(app)}$ for D-glucose uptake in the presence of cytochalasin B is increased 6.3-fold by the presence of 200 mM maltose [$K_{i(app)maltose}$ = 37.7 mM].

DISCUSSION

Inhibitions of human erythrocyte sugar uptake at ice temperature by maltose and cytochalasin B are those expected of inhibitors acting at opposite sides of the membrane (Basketter & Widdas, 1978). Maltose binds at or close to the sugar influx

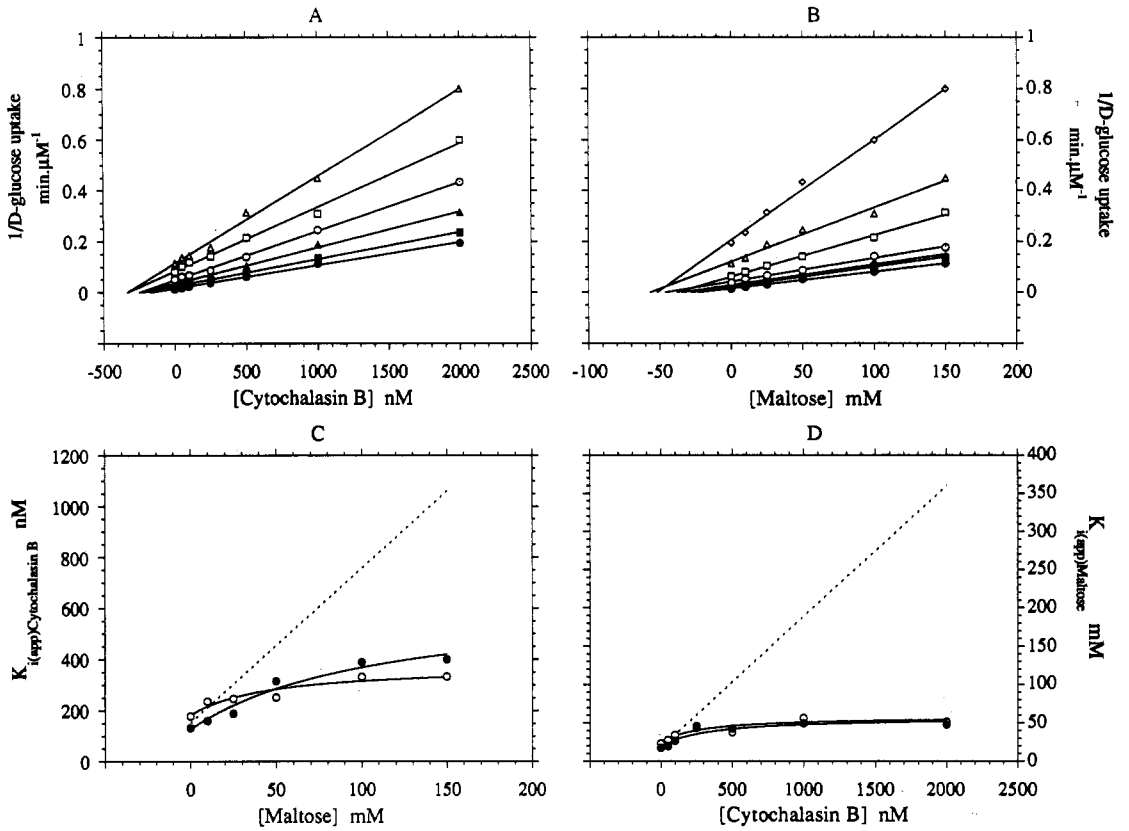

FIGURE 5: Effects of maltose plus cytochalasin B on D-glucose uptake by erythrocytes. This figure summarizes a single experiment in which data points were obtained in duplicate. D-Glucose concentration was 0.1 mM throughout. (A) Effect of maltose on cytochalasin B inhibition of sugar uptake. This is a Dixon plot for inhibition of D-glucose uptake by cytochalasin B. Ordinate: 1/D-glucose uptake in min·μM^{-1}. Abscissa: Cytochalasin B concentration in nM. Uptake was measured in the absence (lowest curve) and presence of increasing maltose levels. These concentrations were 0 (closed circles), 10 mM (closed squares), 25 mM (closed triangles), 50 mM (open circles), 100 mM (open squares), and 150 mM (open triangles). The straight lines drawn through the points were calculated by the method of least squares. The derived $K_{i(app)}$ for cytochalasin B inhibition of uptake ($-x$-intercept) are shown in panel C. (B) Effect of cytochalasin B on maltose inhibition of sugar uptake. Ordinate: As in panel A. Abscissa: Maltose concentration in mM. Uptake was measured in the absence (lowest curve) and presence of increasing cytochalasin B levels. These concentrations were 0 (closed circles), 44 ± 3 nM (closed squares), 97 ± 6 nM (closed triangles), 243 ± 19 nM (open circles), 491 ± 22 nM (open squares), 987 ± 19 nM (open triangles), and 1988 ± 31 nM (open diamonds). The straight lines drawn through the points were calculated by the method of least squares. The derived $K_{i(app)}$ for maltose inhibition of uptake ($-x$-intercept) are shown in panel D. (C) Effect of maltose on $K_{i(app)}$ for cytochalasin B inhibition of D-glucose uptake. Ordinate: $K_{i(app)}$ in nM. Abscissa: As in panel B. Two sets of data points are shown. The open circles represent $K_{i(app)}$ calculated from the Dixon plot shown in panel A. This analysis is heavily weighted by data points obtained at high [cytochalasin B]. The closed circles represent $K_{i(app)}$ calculated by nonlinear regression analysis of the untransformed data in panel A assuming inhibition of transport is characterized by simple hyperbolic kinetics. This analysis is heavily weighted by data points obtained at low [cytochalasin B]. The solid curves were calculated by nonlinear regression according to eq 10. These curves represent the predicted result for a two-site carrier mechanism where K_{M_1} = 181.6 ± 13.5 nM, K_{M_2} = 9 mM, K_2 = 0.069 mM, β = 1, and γ = 2.1 ± 0.3 (open circles; correlation coefficient R = 0.951) or where K_{M_1} = 126.6 ± 12.6 nM, K_{M_2} = 9 mM, K_2 = 0.069 mM, β = 1, and γ = 5.0 ● 1.1 (closed circles; R = 0.980). The dashed curve represents the predicted result for a one-site carrier mechanism (see Theory and Table I for details of assumptions). (D) Effect of cytochalasin B on $K_{i(app)}$ for maltose inhibition of D-glucose uptake. Ordinate: $K_{i(app)}$ in mM. Abscissa: As in panel A. Two sets of data points are shown. The open circles represent $K_{i(app)}$ calculated from the Dixon plot shown in panel B. This analysis is heavily weighted by data points obtained at high [maltose]. The closed circles represent $K_{i(app)}$ calculated by nonlinear regression analysis of the untransformed data in panel B assuming inhibition of transport is characterized by simple hyperbolic kinetics. This analysis is heavily weighted by data points obtained at low [maltose]. The solid curves were calculated by nonlinear regression according to eq 9. These curves represent the predicted result for a two-site carrier mechanism where K_{M_1} = 126 nM, K_{M_2} = 10.0 ± 1.2 mM, K_2 = 0.069 mM, β = 1, and γ = 2.4 ± 0.4 (open circles; R = 0.915) or where K_{M_1} = 126 nM, K_{M_2} = 8.0 ● 0.9 mM, K_2 = 0.069 mM, β = 1, and γ = 2.93 ± 0.55 (closed circles; R = 0.947). The dashed curve represents the predicted result for a one-site carrier mechanism (see Theory and Table I for details of assumptions).

site and thus acts as a competitive inhibitor of sugar uptake. Cytochalasin B binds at or close to the sugar efflux site and acts as a noncompetitive inhibitor of sugar uptake. These results are consistent with both one- and two-site models for sugar transport.

With the two-site model, K_{M_2} (the dissociation constant for maltose binding to the influx site) is obtained from the data of Figures 5 and 6 as

$$K_{M_2} = \frac{K_{i(app)}}{1 + \frac{S_2}{K_2}}$$

in the absence of cytochalasin B. Thus $K_{M_2} \approx 5$ mM. With the simple one-site model, K_{M_2} is obtained in the absence of cytochalasin B as

$$K_{M_2} = \frac{K_{i(app)}k_0}{k_0 + k_{-0} + \frac{S_2}{K_2}(k_0 + k_{-1})}$$

This study does not present sufficient data to provide estimates of the first-order rate constants k_0, k_{-0}, and k_{-1} and the dissociation constant K_2. However, using the values for these constants calculated by Lowe and Walmsley (1986) for D-glucose transport at ice temperature, we estimate $K_{M_2} \approx$ 0.2–0.45 mM.

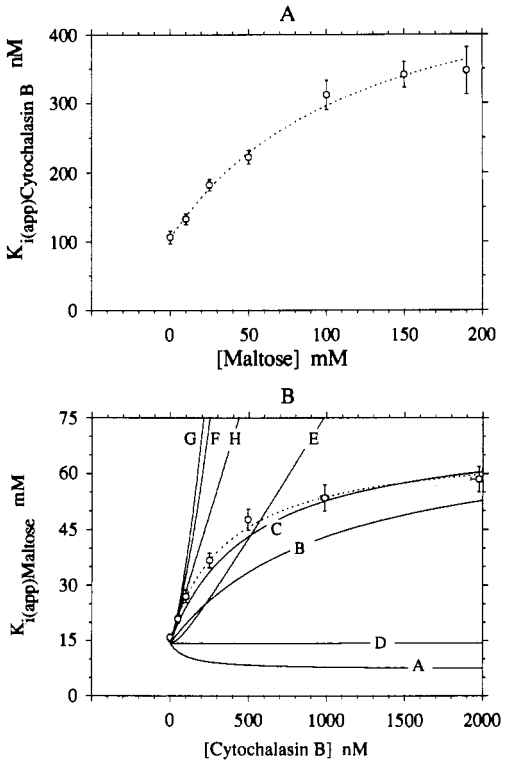

FIGURE 6: Effects of maltose on $K_{i(app)}$ for cytochalasin B inhibition of D-glucose uptake and of cytochalasin B on $K_{i(app)}$ for maltose inhibition of sugar uptake. This figure summarizes 5 separate experiments similar to that shown in Figure 5. $K_{i(app)}$ values were calculated both by Dixon analysis and by nonlinear regression. Data are shown as calculated mean ± 1 standard error. (A) Effects of maltose on $K_{i(app)}$ for cytochalasin B inhibition of D-glucose uptake. Ordinate: $K_{i(app)}$ in nM. Abscissa: Maltose concentration in mM. The dashed curve drawn through the points was calculated according to eq 10 by weighted nonlinear regression. The assumption is that transport is mediated by a two-site carrier. The calculated best fit parameters are the following: K_{M_1} = 105 ± 5 nM, K_{M_2} = 8.8 ● 1.7 mM; γ = 5.1 ± 0.5. β was assumed to be unity, and K_2 = 0.069 mM. The correlation coefficient for the fit is 0.998. (B) Effects of cytochalasin B on $K_{i(app)}$ for maltose inhibition of D-glucose uptake. Ordinate: $K_{i(app)}$ in mM. Abscissa: Cytochalasin B concentration in nM. The dashed curve drawn through the points was calculated according to eq 9 by weighted nonlinear regression. The assumption is that transport is mediated by a two-site carrier. The calculated best fit parameters are the following: K_{M_1} = 83.9 ± 10.3 nM, K_{M_2} = 6.3 ± 0.2 mM; γ = 4.4 ± 0.2. β was assumed to be unity, and K_2 = 0.069 mM. The correlation coefficient for the fit is 0.999. The solid curves were calculated according to eq 13 describing maltose binding to the modified one-site carrier mechanism with the following constants used throughout: K_2 = 10 mM, K_{M_1} = 100 nM, K_{M_2} = 0.4 mM, k_0 = 0.0048 s^{-1}, k_{-0} = 0.089 s^{-1}, and k_{-1} = 8.2 s^{-1}. Curve A: $k_0' = k_0$, $k_{-0}' = k_{-0}$, $\alpha = 1 \rightarrow \infty$, $\beta = 1$, $\gamma = 1$. Curve B: $k_0' = k_0$, $k_{-0}' = k_{-0}$, $\alpha = 1 \rightarrow \infty$, $\beta = 1$, $\gamma = 10$. Curve C: $k_0' = k_0$, $k_{-0}' = k_{-0}$, $\alpha = 1 \rightarrow \infty$, $\beta = 0.5$, $\gamma = 10$. Curve D: $k_0' = k_0$, $k_{-0}' = k_{-0}$, $\alpha = 1 \rightarrow \infty$, $\beta = \infty$, $\gamma = 10$. Curve E: $k_0' = k_{-0}' = 0$, $\alpha = 1$, $\beta = 1$, $\gamma = 1$. Curve F: $k_0' = k_{-0}' = 0$, $\alpha = 1 \rightarrow \infty$, $\beta = 1$, $\gamma = 10$. Curve G: $k_0' = k_{-0}' = 0$, $\alpha = 1 \rightarrow \infty$, $\beta = 0.5$, $\gamma = 10$. Curve H: $k_0' = k_{-0}' = 0$, $\alpha = 1 \rightarrow \infty$, $\beta = \infty$, $\gamma = 10$.

Similar estimates may be obtained by K_{M_1} (the dissociation constant for cytochalasin B binding to the efflux site) in the absence of maltose. The two-site model predicts that

$$K_{M_1} = \frac{K_{i(app)}\left(1 + \frac{S_2}{\beta K_2}\right)}{1 + \frac{S_2}{K_2}}$$

Assuming β is unity (see below), $K_{M_1} \approx 100$ nM. For the simple one-site model

$$K_{M_1} = \frac{K_{i(app)}\left(k_{-0} + \frac{S_2}{K_2}k_{-1}\right)}{k_0 + k_{-0} + \frac{S_2}{K_2}(k_0 + k_{-1})}$$

Thus $K_{M_1} \approx 100$ nM.

These models for transport can be distinguished by analysis of inhibitions of sugar uptake produced by the simultaneous presence of maltose and cytochalasin B. The simple one-site model predicts that $K_{i(app)}$ for maltose inhibition of transport increases monotonically with increasing cytochalasin B concentration (eq 5). Similarly, $K_{i(app)}$ for cytochalasin B inhibition of sugar uptake must increase monotonically with increasing maltose concentration (eq 6). These predicted results were not observed (see Figures 5 and 6). We are, therefore, forced to reject the simple one-site carrier mechanism as an appropriate model for human red cell sugar transport.

The simple one-site carrier mechanism also predicts that high levels of cytochalasin B should completely reverse the ability of maltose to act as a competitive inhibitor of human erythrocyte glucose uptake at ice temperature. This was not observed experimentally (Figure 4) and thus provides a second, albeit less stringent, criterion for rejection of this theoretical mechanism for sugar transport.

While the available data do not prove that transport is mediated by a two-site mechanism, it is of interest to analyze these results within the context of such a model. The data of Figure 6 have been analyzed according to eqs 9 and 10, which describe the effects of a trans inhibitor on $K_{i(app)}$ for inhibition of two-site carrier-mediated transport by an inhibitor acting at one side of the membrane. The data sets were analyzed by weighted nonlinear regression to obtain estimates of the cooperativity factor γ. γ describes interactions between the internal and external binding sites when they are occupied by nontransported inhibitors. We assumed that the cooperativity factor β was unity. β describes interactions between the internal and external binding sites when one site is occupied by a transported sugar and the second by a nontransported inhibitor. The use of a β cooperativity factor of unity appears justified for three reasons. $K_{d(app)}$ for cytochalasin B binding to the glucose carrier of red cell ghosts at ice temperature (145 ± 7 nM; Helgerson & Carruthers, 1987) is unaffected by the presence of D-glucose at the exterior of the cell (Helgerson & Carruthers, 1987). $K_{m(app)}$ for D-glucose uptake is unaffected by cytochalasin B (Figure 4), and $K_{i(app)}$ for cytochalasin B inhibition of red cell D-glucose uptake (122 ± 11 nM) is unaffected by increasing extracellular D-glucose.

The curves drawn through the data points in Figure 6 represent the computed best fits of the data. In both instances (maltose modulation of cytochalasin B inhibition of transport and cytochalasin B modulation of maltose inhibition of transport), the cooperativity factor γ is approximately 4.5. Interpreted within the context of the two-site model, this means that maltose and cytochalasin B binding sites display negative cooperatively. In a previous study of maltose inhibition of cytochalasin B binding to the glucose carrier of red cells and red cell ghosts we estimated tht γ = 3.8 ± 0.1 (Helgerson & Carruthers, 1987). Thus the ligand binding and sugar transport studies are in quantitative agreement.

We conclude that the characteristics of human erythrocyte D-glucose uptake inhibition by the simultaneous presence of nontransported inhibitors acting at the inside and outside of the cell are inconsistent with the predictions of the simple one-site carrier model for sugar transport. Rather, the data suggest that maltose and cytochalasin B binding sites exist

simultaneously in the glucose carrier and that these sites display negative cooperativity when occupied.

A remaining caveat is the question of whether or not maltose and cytochalasin B binding sites represent sugar influx and sugar efflux sites, respectively. Studies of substrate protections (by cytochalasin B or maltose) and enhancements (by intra- plus extracellular D-glucose) of irreversible inhibitions of sugar transport by halodinitrobenzenes suggest that the sugar efflux and cytochalasin B binding sites may not be identical. Rather, these sites may be overlapping or mutually exlusive sites (Krupka, 1971; Barnett et al., 1975). Thus it is possible that cytochalasin B could remain bound to a one-site carrier even when the sugar influx site is occupied by maltose or D-glucose.

We consider such a modified one-site carrier under Theory (see above and Figure 3). This modified one-site carrier model can (with a suitable choice of constants) predict the effects of cytochalasin B on $K_{d(app)}$ for maltose binding to the carrier (see Figure 6). However, by use of the values assigned to these constants in order to mimic the effects of cytochalasin B on $K_{d(app)}$ for maltose binding to the carrier, this model predicts that, in the absence of maltose, cytochalasin B will be without effect on or even *increase* V_{max} for sugar uptake. This prediction is incompatible with the transport data and forces rejection of the modified one-site carrier model.

We conclude that simple and modified one-site carrier mechanisms for sugar transport are unable to account for inhibitions of sugar uptake produced by the simultaneous presence of cytochalasin B and maltose. A two-site carrier mechanism in which sugar influx and sugar efflux sites coexist is consistent with the experimental data.

Registry No. Glucose, 50-99-7.

REFERENCES

Appleman, J. R., & Lienhard, G. E. (1989) *Biochemistry 28*, 8221–8227.

Baker, G. F., & Widdas, W. F. (1973a) *J. Physiol. (London) 231*, 143–165.

Baker, G. F., & Widdas, W. F. (1973b) *J. Physiol. (London) 231*, 129–142.

Baker, G. F., Basketter, D. A., & Widdas, W. F. (1978) *J. Physiol. (London) 278*, 377–388.

Barnett, J. E. G., Holman, G. D., Chalkey, R. A., & Munday, K. A. (1975) *Biochem. J. 145*, 417–429.

Basketter, D. A., & Widdas, W. F. (1978) *J. Physiol. 278*, 389–401.

Carruthers, A. (1986a) *Biochemistry 25*, 3592–3602.

Carruthers, A. (1986b) *J. Biol. Chem. 261*, 11028–11037.

Carruthers, A. (1989) in *The Red Cell Membrane* (Raess, B U., & Tunnicliff, G., Eds.) pp 249–279, Humana Press, Clifton, NJ.

Carruthers, A. (1991) *Biochemistry* (preceding paper in this issue).

Gorga, F. R., & Lienhard, G. E. (1981) *Biochemistry 20*, 5108–5113.

Gorga, F. R., & Lienhard, G. E. (1982) *Biochemistry 21*, 1905–1908.

Helgerson, A. L., & Carruthers, A. (1987) *J. Biol. Chem. 262*, 5464–5475.

Holman, G. D. (1980) *Biochim. Biophys. Acta 599*, 202–213.

Holman, G. D., Busza, A. L., Pierce, E. J., & Rees, W. D. (1981) *Biochim. Biophys. Acta 649*, 503–514.

Jung, C. Y., & Rampal, A. L. (1976) *Fed. Proc. 35*, 780.

Jung, C. Y., & Rampal, A. L. (1977) *J. Biol. Chem. 252*, 5456–5463.

Krupka, R. M. (1971) *Biochemistry 10*, 1143–1153.

Krupka, R. M. (1985) *J. Membr. Biol. 83*, 71–80.

Krupka, R. M., & Devês, R. (1981) *J. Biol. Chem. 256*, 5410–5416.

Lowe, A. G., & Walmsley, A. R. (1986) *Biochim. Biophys. Acta 857*, 146–154.

Lowe, A. G., & Walmsley, A. R. (1987) *Biochim. Biophys. Acta 903*, 547–550.

Naftalin, R. J. (1988a) *Biochim. Biophys. Acta 946*, 431–438.

Naftalin, R. J. (1988b) *Trends Biochem. Sci. 13*, 425–426.

Naftalin, R. J., & Holman, G. D. (1977) in *Membrane transport in red cells* (Ellory, J. C., and Lew, V. L., Eds.) pp 257–300, Academic Press, New York.

Naftalin, R. J., Smith, P. M., & Roselaar, S. E. (1985) *Biochim. Biophys. Acta 820*, 235–249.

Sogin, D. C., & Hinkle, P. C. (1980) *Biochemistry 19*, 5417–5420.

Stein, W. D. (1986) in *Transport and diffusion across cell membranes*, pp 231–305, Academic Press, New York.

Wheeler, T. J. (1986) *Biochim. Biophys Acta 862*, 387–398.

Wheeler, T. J., & Hinkle, P. C. (1981) *J. Biol. Chem. 256*, 8907–8914.

Wheeler, T. J., & Hinkle, P. C. (1985) *Annu. Rev. Physiol. 47*, 503–518.

Wheeler, T. J., & Whelan, J. D. (1988) *Biochemistry 27*, 1441–1446.

Widdas, W. F. (1952) *J. Physiol. (London) 118*, 23–39.